Manufacturing Technologies and Applications
MATECA

Pack Aluminizing of Zirconium 702 Alloy to Improve Surface Hardness and Wear Resistance

Faiz Muhaffel[1,*]

[1]*Department of Metallurgical and Materials Engineering, Chemical and Metallurgical Engineering Faculty, Istanbul Technical University, Istanbul, Türkiye*

ABSTRACT

Zirconium 702 (Zr 702) alloy exhibits excellent corrosion resistance but suffers from low hardness and poor wear resistance, limiting its use in wear-intensive applications. In this study, a pack aluminizing treatment was applied to Zr 702 to form a hard aluminide surface layer aimed at improving its tribological performance. Characterization by X-ray diffraction (XRD) and cross-sectional scanning electron microscopy/energy-dispersive spectroscopy (SEM/EDS) confirmed the formation of a continuous diffusion coating approximately 40 µm thick, composed predominantly of an Al-rich intermetallic phase (mainly Al_3Zr). This aluminized layer was dense, well-adhered, and significantly harder than the substrate, with a Vickers microhardness of 703.1 ± 76.7 HV0.025 compared to 182.9 ± 20.7 HV0.025 for untreated Zr 702. In dry sliding reciprocating wear tests (2–4 N loads against an alumina counterface), the aluminized sample exhibited a much lower and more stable coefficient of friction (COF), reaching a steady value of about 0.35 under 4 N load, whereas the untreated Zr 702 stabilized around 0.6 under the same conditions. In comparison with the untreated Zr 702, the aluminized surface exhibited about a 70% reduction in wear volume under a 4 N load as a result of the improved hardness and modification of its surface with an intermetallic layer. Wear track analysis further revealed that the dominant wear mechanism shifted from severe adhesive and abrasive wear in the untreated Zr 702 to a mild abrasive/oxidative wear mode in the aluminized sample, as the hard intermetallic layer protected the underlying Zr from significant damage. Overall, the pack aluminizing process remarkably enhanced the surface hardness, frictional behavior, and wear resistance of Zr 702, demonstrating an effective surface engineering approach to improve the tribological performance of zirconium alloys.

Keywords: *Zirconium, Thermo-chemical diffusion treatment, Aluminising, Microstructure, Hardness, Wear resistance*

702 Zirkonyum Alaşımının Yüzey Sertliğini ve Aşınma Direncini Artırmaya Yönelik Kutu Alüminizasyon Uygulaması

ÖZET

Zirkonyum 702 (Zr 702) alaşımı mükemmel korozyon direnci sergilemekle birlikte düşük sertlik ve zayıf aşınma direnci nedeniyle yoğun aşınma koşullarındaki uygulamalarda sınırlı kullanılmaktadır. Bu çalışmada, Zr 702'ye kutu aluminizasyonu işlemi uygulanarak tribolojik performansını artırmayı amaçlayan sert bir aluminit yüzey tabakası oluşturulmuştur. X-ışını kırınımı (XRD) ile taramalı elektron mikroskoskopisi/enerji dağılımlı spektroskopisi (SEM/EDS) karakterizasyonu, ağırlıklı olarak Al'ce zengin bir intermetalik fazdan (başlıca Al_3Zr) oluşan, yaklaşık 40 µm kalınlığında bir difüzyon esaslı kaplamanın oluştuğunu doğrulamıştır. Bu tabaka yoğun, altlığa iyi yapışmış ve iç yapıdan belirgin şekilde daha serttir. Kaplamanın Vickers mikrosertliği 703,1 ± 76,7 HV0.025 olup, işlem görmemiş Zr 702'nin sertliği ise 182,9 ± 20,7 HV0.025 mertebesindedir. Kuru kaymalı geri-ileri aşınma testlerinde (2–4 N yük, alümina karşı yüzey) aluminizasyon uygulanmış numune çok daha düşük ve kararlı bir sürtünme katsayısına (COF) ulaşmış ve COF değeri 4 N yük altında yaklaşık 0,35 düzeyinde sabitlenirken işlem görmemiş Zr 702 aynı koşullarda yaklaşık 0,6'da stabilize olmuştur. Artan sertlik ve yüzeyin sert intermetalik bir tabaka ile modifiye edilmesi sayesinde, aluminizasyon uygulanmış yüzey 4 N yükte aşınma hacmini işlem görmemiş Zr 702'ye göre yaklaşık %70 oranında azaltmıştır. Aşınma izi analizleri, işlen görmemiş Zr 702'de gözlenen şiddetli adezif ve abrazif aşınma mekanizmalarının aluminizasyon uygulanmış numunede sert intermetalik tabakanın altlık Zr 702'yi koruması sayesinde hafif aşındırıcı/oksidatif aşınmaya dönüştüğünü ortaya koymuştur. Sonuç olarak, kutu aluminizasyonu işlemi Zr 702'nin yüzey sertliğini, sürtünme davranışını ve aşınma direncini dikkate değer ölçüde iyileştirerek zirkonyum alaşımlarının tribolojik performansını artırmak için etkili bir yüzey mühendisliği yaklaşımı sunmaktadır.

Anahtar Kelimeler*: Zirkonyum, Termo-kimyasal difüzyon işlemi, Alüminizasyon, Mikroyapı, Sertlik, Aşınma direnci*

*Corresponding author, e-mail: muhaffel@itu.edu.tr

Received 05.06.2025; Revised 22.07.2025; Accepted 11.08.2025
https://doi.org/10.52795/mateca.1715207
To cite this article: F. Muhaffel, Pack Aluminizing of Zirconium 702 Alloy to Improve Surface Hardness and Wear Resistance, Manufacturing Technologies and Applications 6(2) (2025) 227-238.

1. INTRODUCTION

Zirconium and its alloys are important engineering materials recognized for their corrosion resistance and unique nuclear properties [1]. Due to their low thermal neutron absorption cross-section and stability in high-temperature water environments, zirconium-based alloys (such as Zircaloys) are widely used in the nuclear industry as fuel cladding and structural components in nuclear reactors [1,2]. As a result of their biocompatibility and ability to produce a hard, wear-resistant oxide surface, zirconium alloys have gained interest for use in surgical implants and medical devices, such as oxidized zirconium alloys employed in artificial joint components [3,4]. Additionally, zirconium is considered for specific components in the aerospace and chemical process industries that must withstand corrosive media and high temperatures. Although zirconium has many advantages and is used in various applications, its relatively low hardness poses a significant challenge [5]. Zirconium surfaces are, therefore, susceptible to scratching, galling, and wear when exposed to friction or abrasion [6]. This poor wear resistance can lead to failure or high maintenance needs in applications where moving parts or contact surfaces involve zirconium and its alloys.

Zirconium is not suitable for use in load-bearing or high-wear applications due to its inherently low hardness and tendency to wear. For example, zirconium alloy cladding tubes in nuclear reactors may experience fretting wear at contact points [7], and any articulating surface in biomedical implants must resist wear to prevent the generation of debris [8]. Thus, improving the hardness and wear resistance of zirconium is crucial for enhancing its performance and reliability. There are several material engineering strategies that can be employed in order to overcome this issue. It is possible to increase the strength and hardness of zirconium by bulk alloying and heat treating, or by adjusting the alloy composition. However, bulk hardening is often limited because the addition of too many alloying elements can compromise zirconium's corrosion resistance or neutron transparency. Additionally, zirconium's HCP crystal structure limits the phase transformations for traditional hardening (unlike steel's martensitic transformation). Thus, surface modification techniques are more advantageous since they allow the surface properties to be enhanced without affecting the beneficial bulk properties of the zirconium.

Surface engineering of zirconium typically involves creating a hardened layer or coating on the surface of the material that is durable and can withstand wear and contact, thus protecting the underlying substrate. The most common methods are thermochemical treatments (such as nitriding [9] or oxidation [10]) and surface coatings (such as physical vapor deposition of hard ceramic films [11] or cold spray coatings [12]). Surface hardness can be improved in varying degrees by each of these methods. As an example, when zirconium is nitrided, nitrogen is introduced into the surface to form zirconium nitride (ZrN), a very hard ceramic compound. Similarly, the thermal oxidation process can produce a thin layer of zirconium oxide (ZrO_2), which is hard and wear-resistant (this principle is used in oxidized zirconium orthopedic implants). In a recent study, Xiong et al. [13] applied a catalytic ceramic conversion treatment to zirconium 702 alloy using noble metal catalysts, resulting in the formation of a dense ZrO_2-based oxide layer that significantly enhanced hardness and reduced wear rate and friction. In another study, Guan et al. [6] applied a Cr–Nb–Ti–Zr alloy coating via laser cladding to Zr702, resulting in a duplex structure with improved hardness and enhanced tribological performance. Despite the high hardness of such treatments, they often produce ceramic layers that are brittle or must be controlled carefully to avoid cracking. Furthermore, applied surface coatings (such as PVD coatings of TiN or diamond-like carbon) may provide extreme hardness but may be affected by adhesion problems or mismatches in mechanical properties.

Among the various surface modification techniques, aluminizing, which involves alloying the metal surface with aluminum, has emerged as a promising method for improving the surface properties of many metals and metallic alloys [14–16]. In the case of aluminizing as a thermo-chemical diffusion treatment, the surface of zirconium is enriched with aluminum, allowing diffusion and reaction to occur at elevated temperatures and forming intermetallic compounds of zirconium and aluminum. These zirconium aluminide phases are significantly harder than the base metal and can act as a durable protective layer. In contrast to brittle ceramic coatings, intermetallic layers can exhibit good adhesion (as they are grown from the substrate) and have a graded composition that can reduce the risk of spalling between the hard surface and the softer core. Moreover, aluminized surfaces are well-known for their excellent oxidation resistance at high temperatures as they readily form a stable alumina (Al_2O_3) scale [17].

Pack aluminizing, a promising thermo-chemical diffusion treatment known for creating adherent intermetallic layers with superior hardness, has been successfully applied to many metallic alloys but has not yet been investigated for zirconium alloys. To address this research gap, the present study provides a detailed investigation of the aluminizing process applied specifically to zirconium 702 (Zr 702) alloy, focusing on the microstructural changes and enhancements in surface hardness and tribological behavior. Therefore, the microstructural features were examined using optical and scanning electron microscopy techniques, and the

thickness of the aluminized layer was measured. To reveal the mechanical and tribological properties, the hardness of the aluminized layer was determined using micro-Vickers tests and the wear resistance was calculated and compared with that of the untreated Zr 702 through reciprocating dry sliding wear tests under varying loads at room temperature. The results of this study revealed that aluminizing effectively minimizes the surface limitations of zirconium, thereby enabling its broader application in harsh conditions, and to the best of the author's knowledge, this is the first successful attempt and investigation of an aluminized layer on zirconium.

2. MATERIAL AND METHOD

2.1 Aluminizing Process

In the present study, the pack-aluminizing technique was applied to zirconium 702 alloy disc specimens with a diameter of 16 mm and a thickness of 4 mm. Prior to the coating process, the discs were first ground with silicon carbide (SiC) abrasive paper of P400 grit to obtain a uniformly smooth surface. They were then washed thoroughly in ethanol to remove residual particles, followed by air-drying at ambient room temperature. The aluminizing pack consisted of 25 wt.% aluminum powder (aluminum source), 5 wt.% aluminum-trichloride ($AlCl_3$) as the halide activator, and 70 wt.% alumina (Al_2O_3) acting as an inert filler. A layer of this blended powder, approximately 2 cm thick, was placed at the bottom of a stainless-steel container. The pre-prepared specimen was positioned on this layer, ensuring full contact with its lower surface, then the remaining volume of the container was completely filled and compacted with the same powder mixture before sealing. Diffusion treatment was performed in a conventional laboratory furnace under atmospheric conditions at 700 °C for a duration of 4 h to promote aluminum migration and intermetallic layer formation. Hereafter, the coated sample is referred to as Zr–Al sample, whereas the uncoated sample is referred to as the untreated Zr 702.

2.2. Microstructural Characterization

The phase composition of the substrate and the aluminized layer was analyzed using a Cu-Kα X-ray diffractometer (Philips PW-3710) operated at 40 kV and 40 mA. Diffraction patterns were collected over a 2θ range of 20° to 80°, with a step increment of 0.020° and a scanning rate of 1° min^{-1} to provide adequate resolution for identifying both the substrate and aluminized layer constituents. Surface topography and cross-sectional microstructure were investigated using scanning electron microscopy (SEM, Hitachi TM-1000 and Thermo Scientific Quattro S). To quantify the chemical composition and to demonstrate elemental distribution within the aluminized layer, energy-dispersive X-ray spectroscopy (EDS, Oxford Instruments) mapping was performed. Coating thickness was assessed by light optical microscopy (Leica ICC50 HD). Ten independent thickness measurements were taken at randomly selected locations, and the mean value along with its standard deviation was calculated.

2.3. Hardness and Wear Tests

Hardness measurements were conducted on polished cross-sections using a 25 g load (HV0.025) by a Vickers microhardness tester (Wilson Tukon 1102). A total of ten indents were placed at least three diagonals apart in order to avoid cross-influence, and a mean and standard deviation were calculated. Before tribological testing, all samples were ground with P2500 SiC paper to minimize initial surface roughness. Reciprocating wear tests were performed on a linear oscillation tribometer (Tribotech) at room temperature. An alumina counter-body, 6 mm in diameter, traversed a 5 mm stroke length on each sample at a sliding speed of 10 mm s^{-1}. Normal loads of 2, 3, and 4 N were applied, and each test proceeded until a cumulative sliding distance of 50 m was achieved. The tribometer's software continuously monitored the coefficient of friction (COF). After completion of each test, worn tracks were visualized via light optical microscopy and SEM (Hitachi TM-1000) to examine damage mechanisms. Specific wear rates were determined by measuring two-dimensional cross-sectional profiles of the tracks with a stylus contact profilometer (Veeco Dektak 6M).

3. EXPERIMENT AND RESULTS

3.1 Phase Composition and Coating Microstructure

The XRD spectra of untreated Zr 702 and Zr-Al samples plotted in Figure 1 revealed distinct phase transformations induced by the aluminizing treatment. The untreated Zr 702 substrate showed reflections characteristic of α-Zr (hexagonal close-packed structure). In contrast, after aluminizing, new diffraction peaks

appeared, corresponding to a zirconium–aluminum intermetallic compound. Specifically, peaks matching Al_3Zr were evident, indicating the formation of this phase in the formed aluminized layer. No distinct pure aluminum phase was detected, indicating that the aluminum has fully diffused into the substrate to form an intermetallic layer. These XRD results (Figure 1) confirmed that the aluminizing process successfully produced a multi-phase Zr–Al intermetallic coating. This is in agreement with studies on diffusion couple systems, in which Al_3Zr is the primary phase in the Zr–Al system [18,19]. The formation of such intermetallic phases is crucial, as they are significantly harder than the base metal. For example, bulk Al_3Zr can exhibit a microhardness on the order of 600 HV or higher [20], whereas unalloyed Zr is relatively soft (typically ~140–160 HV) [21].

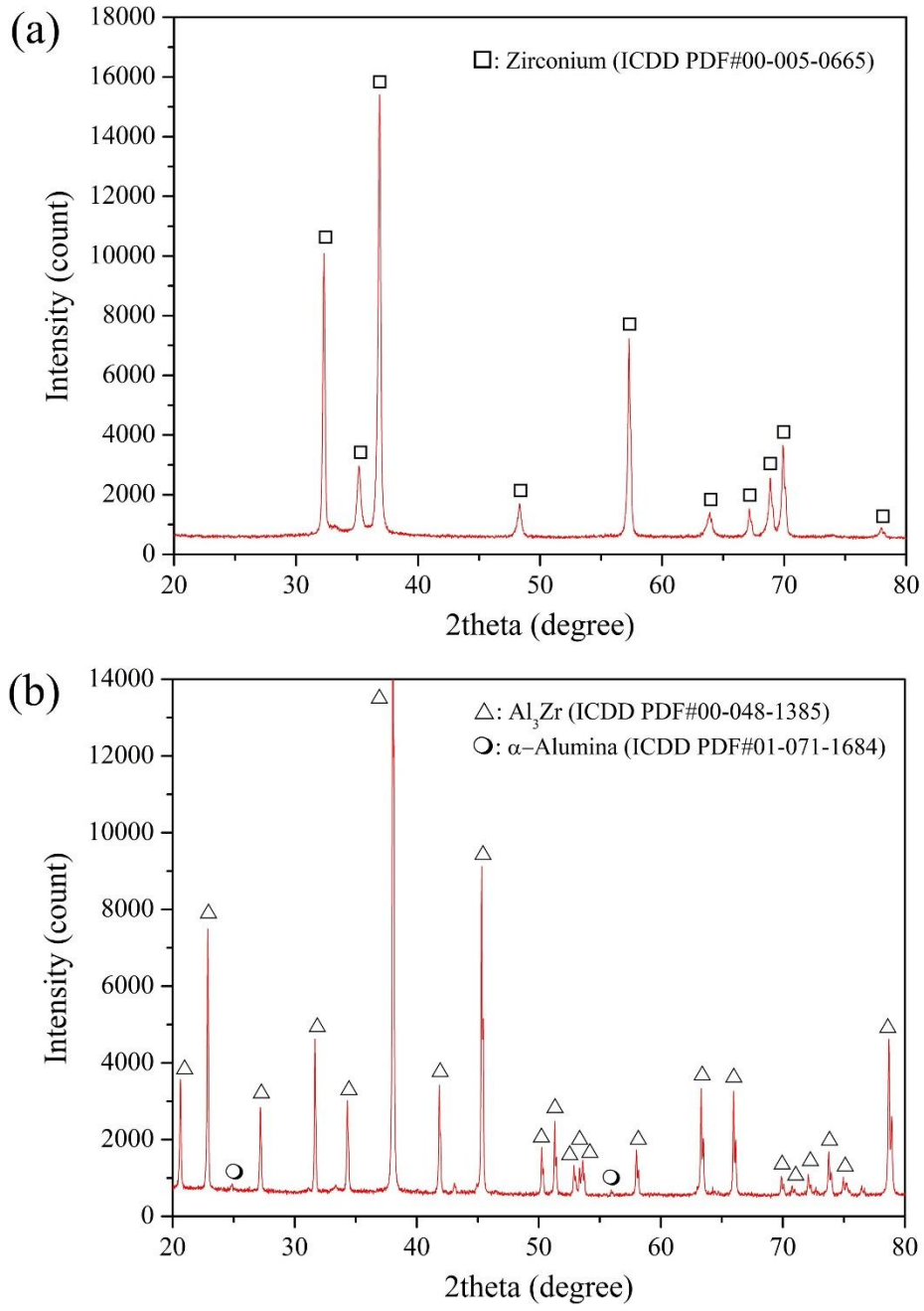

Figure 1. XRD spectrum of (a) untreated Zr 702 and (b) Zr-Al samples.

Cross-sectional SEM micrographs presented in Figure 2(a-b) showed a uniform aluminized layer covering the Zr 702 substrate. The coating was relatively dense and well-adherent, with no visible cracks. Only some voids were observed in the aluminized layer, especially at higher magnification during SEM investigations. However, no voids were detected at the interface between the aluminized layer and the Zr 702 substrate, which indicated a good bonding. The average thickness of the aluminized layer was measured to be 39.81 ± 3.57 µm across multiple cross-sections, indicating a substantial diffusion zone. This thickness suggested that the pack

aluminizing process allowed aluminum to penetrate to a depth sufficient for forming a protective layer. Backscattered electron imaging showed that the coating formed a continuous diffusion layer. EDS analysis of the circled aluminized layer region (Figure 2c) demonstrated 67.6 ± 0.6 at.% Al, 26.1 ± 0.6 at.% Zr, 6.1 ± 1.2 at.% O, and 0.2 ± 0.1 at.% Fe. The Al/Zr ratio (~2.6) approaches the Al_3Zr stoichiometry (3:1), confirming that the aluminized layer was dominated by an Al-rich zirconium aluminide, which was consistent with the dominant Al_3Zr reflections observed in XRD. Oxygen detection suggested minor alumina or subsurface oxidation [17], while the negligible Fe content was attributed to the chemical composition of the Zr 702 substrate and was insufficient to influence phase constitution. Overall, the EDS data confirmed effective diffusion of aluminum and the formation of an intermetallic coating enriched in aluminum relative to zirconium.

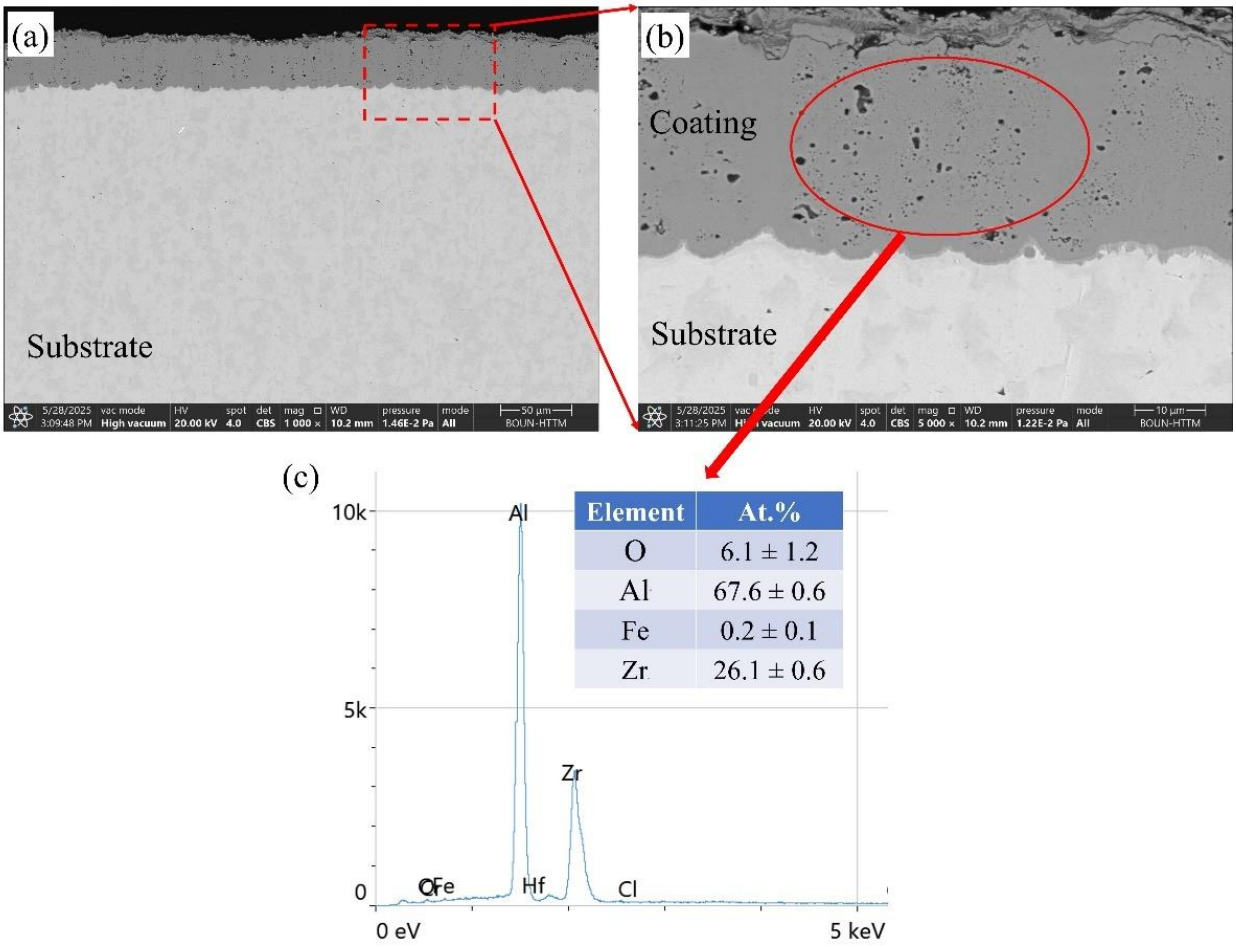

Figure 2. (a) Cross-section SEM micrograph of the Zr–Al sample, (b) higher magnification SEM micrograph of the aluminized layer and (c) EDS analysis results of the aluminized layer on Zr 702 substrate.

EDS elemental maps (Figure 3) corroborated this structure, which revealed a high concentration of aluminum in the aluminized layer and a sharp compositional gradient at the interface. This elemental distribution confirmed the formation of Zr–Al intermetallic compounds throughout the ~40 µm surface layer, with minimal aluminum diffusion beyond that depth. The EDS analysis also detected no significant oxygen within the coating, which suggested that the pack aluminizing process (conducted in a closed container) minimized oxide formation; therefore, the intermetallic layer was predominantly composed of the intended intermetallic phase. The presence of a dense, Al-rich intermetallic layer was a distinctive feature of successful aluminizing and was expected to impart high hardness and good load-bearing capacity to the surface [22–24]. Similarly, Gürol et al. [25] also used halide-activated pack aluminizing treatment on ER307 stainless steel to produce hard coatings (nano-hardness up to ~14 GPa).

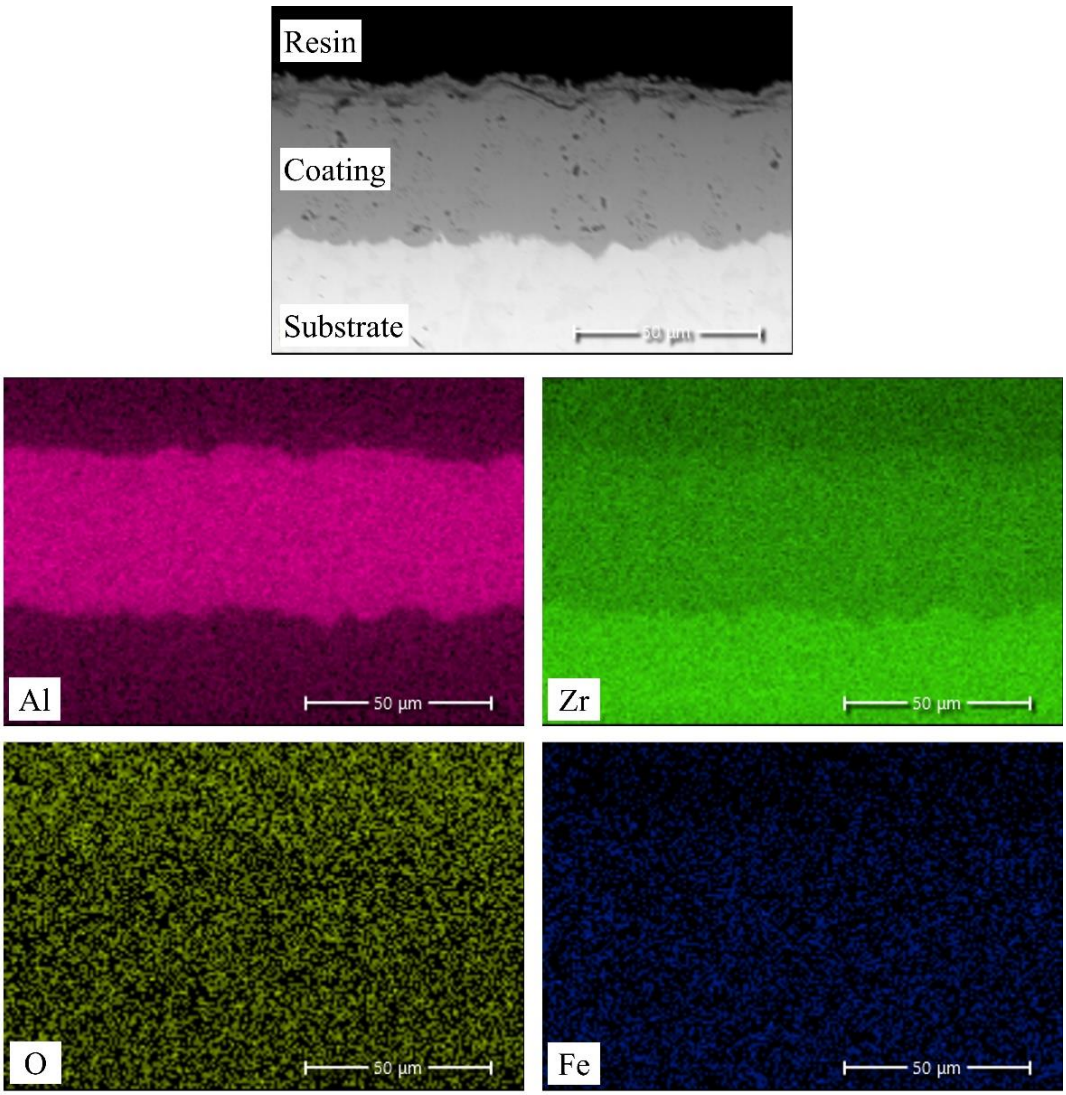

Figure 3. EDS mapping and elemental distribution on the cross-section of the Zr-Al sample.

3.2. Hardness, Wear and Friction Performance

Vickers microhardness tests confirmed a surface hardness of 703.1 ± 76.7 HV0.025 for the aluminized layer, whereas the untreated substrate was measured as 182.9 ± 20.7 HV0.025, evidencing a nearly 4 times increase in hardness. Reciprocating wear tests were performed on both untreated Zr 702 and Zr–Al samples under normal loads of 2, 3, and 4 N. The evolution of the COF during these tests is presented in Figure 4. All tests began with a running-in period where the COF rose to a steady-state value. However, the magnitude and stability of the COF differed markedly between the untreated Zr 702 and Zr–Al samples. The untreated Zr sample consistently exhibited a higher friction coefficient and greater fluctuation. For instance, at 2 N load, the steady-state COF for untreated Zr hovered around ~0.5–0.6 (with noise in the friction signal due to surface damage and material transfer), whereas the Zr–Al sample stabilized at a lower COF, roughly in the ~0.3–0.4 range, with a smoother sliding response. This trend became more pronounced at higher loads. Under 4 N load, the COF of the uncoated Zr sample spiked intermittently and averaged above 0.6 (often punctuated by sudden increases, indicative of stick-slip or severe adhesive events).

In contrast, the Zr–Al sample at 4 N maintained a comparatively lower COF (~0.35) with much smaller oscillations. The overall lower friction of the aluminized layer can be attributed to its harder surface and altered wear mechanism. The higher hardness of the intermetallic layer reduced the real contact area and suppressed adhesive junction formation, directly accounting for the lower and more stable friction response observed for the Zr–Al sample. Moreover, any wear debris generated from the Zr–Al sample was likely composed of brittle intermetallic or oxidized particles that do not adhere strongly and can potentially act as third-body lubricants. Additionally, the formation of lubricious oxide tribofilms (Al_2O_3 or ZrO_2) during sliding may play a role in further reducing the COF under unlubricated conditions.

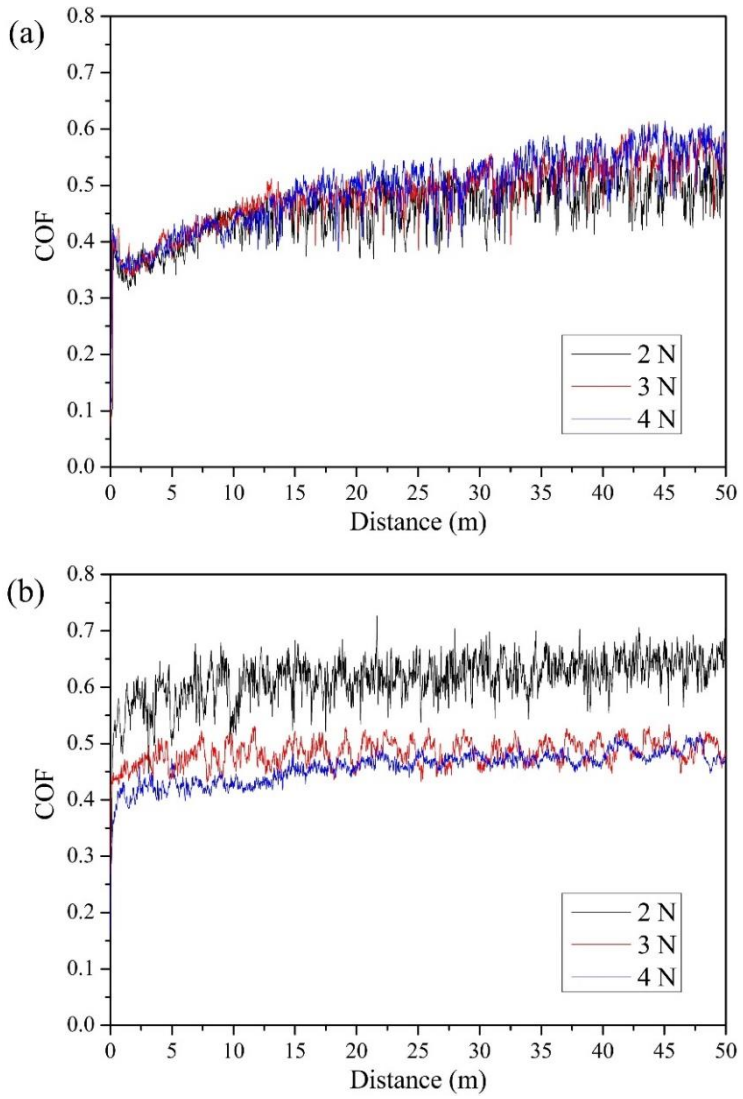

Figure 4. Friction curves of (a) the untreated Zr 702 and (b) Zr-Al samples under sliding 2, 3 and 4 N of loads.

According to the quantitative wear results (Table 1), the volumetric wear loss of the Zr–Al sample is only a small fraction of that of the untreated Zr sample under all tested loads. For example, at 4 N, the untreated Zr sample suffered large-scale material removal, whereas the Zr-Al sample had approximately 3 times less volumetric wear loss. This corresponds to a reduction in wear volume by roughly 70% for the aluminized sample relative to the untreated Zr sample at the highest load. Although both materials exhibited lower wear under 2 N loads, the Zr–Al sample consistently outperformed, with significantly smaller wear scars.

Table 1. Results of reciprocating wear tests of the untreated Zr and Zr-Al samples for 2, 3 and 4 N of loads.

Sample	Testing load (N)	Wear volume loss (mm^3)	Wear rate (mm^3/Nm)	Mean COF	Maximum COF
Untreated Zr 702	2	65.05×10^{-3}	0.650×10^{-3}	0.458	0.573
	3	89.03×10^{-3}	0.593×10^{-3}	0.488	0.613
	4	106.55×10^{-3}	0.532×10^{-3}	0.495	0.615
Zr-Al	2	24.27×10^{-3}	0.243×10^{-3}	0.617	0.727
	3	35.58×10^{-3}	0.237×10^{-3}	0.484	0.534
	4	38.01×10^{-3}	0.190×10^{-3}	0.458	0.518

The wear track profiles measured by 2D profilometry are illustrated in Figure 5. In the case of untreated Zr, the wear tracks were deep and broad, indicating a severe penetration into the soft substrate. In contrast, the tracks on the Zr–Al sample were much shallower and narrower. At 4 N, the track depth of the untreated Zr sample reached over 25 µm, whereas the Zr-Al sample had a relatively lower depth (about 15-16 µm), not penetrating the aluminized layer. These profile results confirmed that ~40 µm intermetallic layer remained through the tests, and even under the harsh 4 N sliding load condition, it prevented catastrophic wear of the substrate. The substantial reduction in wear can be attributed to the high hardness and strength of the intermetallic layer, which distributed contact stresses and resisted cutting or ploughing by the alumina counterface. As a result, the aluminized layer served as a sacrificial coating, which prevented gross deformation of the ductile Zr underneath. It has been shown that TiN coatings on Zircaloy reduce wear volume by factors of 2–3 by taking on the wear damage themselves (by means of brittle micro-fracture) before the substrate is affected [26]. The Zr-Al intermetallic layer in the present study exhibited similar behavior, withstanding the impact of wear and thereby significantly extending component's life.

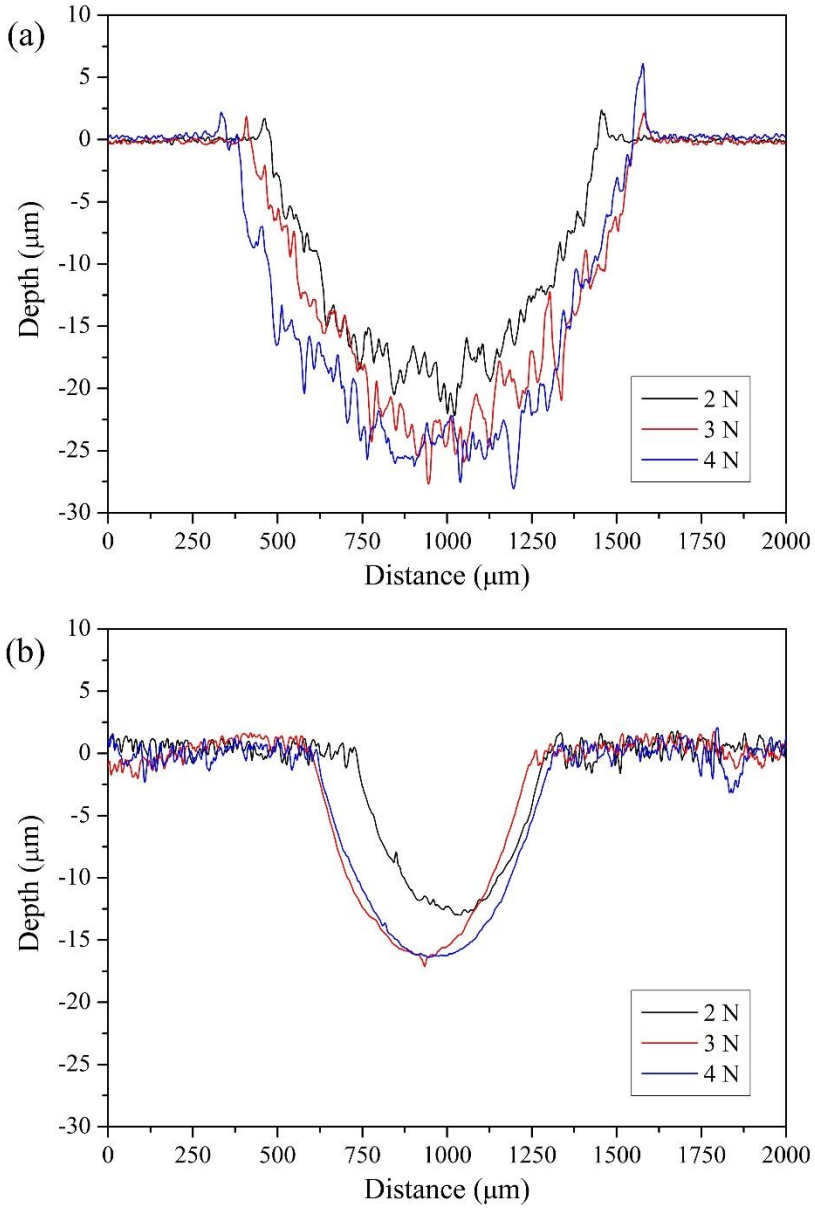

Figure 5. 2D profiles of the wear track of (a) untreated Zr 702 and (b) Zr-Al samples under sliding 2, 3, and 4 N of loads.

The morphology of the wear tracks observed via SEM is shown in Figure 6. The wear track on the untreated Zr at a 4 N load was characterized by severe damage, which consisted of long and deep grooves aligned with the sliding direction, as well as patches of adhered debris. These features are characteristics of abrasive–adhesive wear. Abrasive grooves indicated hard asperities or debris ploughing the soft Zr surface, while the

smeared areas suggested material transfer (adhesion) between the Zr 702 substrate and the alumina ball. The combination of these mechanisms resulted in significant material removal in the uncoated Zr sample. Chunks of metal appeared to have been torn from the surface, and some of this material was transferred to the counterface, while other pieces remained as loose debris.

In contrast, the wear track on the Zr–Al sample, which has an aluminized layer on its surface, was markedly different. At 4 N, the wear track of the Zr–Al showed only shallow fine scratches with a much more uniform appearance. The layer remained continuous, with no evidence of gross spallation or delamination observed in the SEM micrographs from the wear tests conducted under 2 and 3 N. Only at 4 N does the coated track show small chipped regions, indicating that wear has begun to fracture the intermetallic layer locally. However, there were no large peeled-off areas. The overall worn surface of the Zr–Al was relatively smooth and free of deep grooves for all the load conditions. Any debris generated from the coated surface was likely to be fragmented intermetallic particles or oxides, which tended to be harder but also more brittle, as they acted as micro-abrasives that polished the sliding track rather than adhering and causing severe ploughing. Indeed, the transition from an adhesive/delamination wear regime on the untreated Zr sample to an abrasive/oxidative wear regime on the Zr-Al sample was a fundamental reason for the improved performance. This shift was clearly evidenced by SEM investigations as the wear tracks of the Zr-Al sample lacked the prominent plastic deformation features seen on the untreated Zr sample.

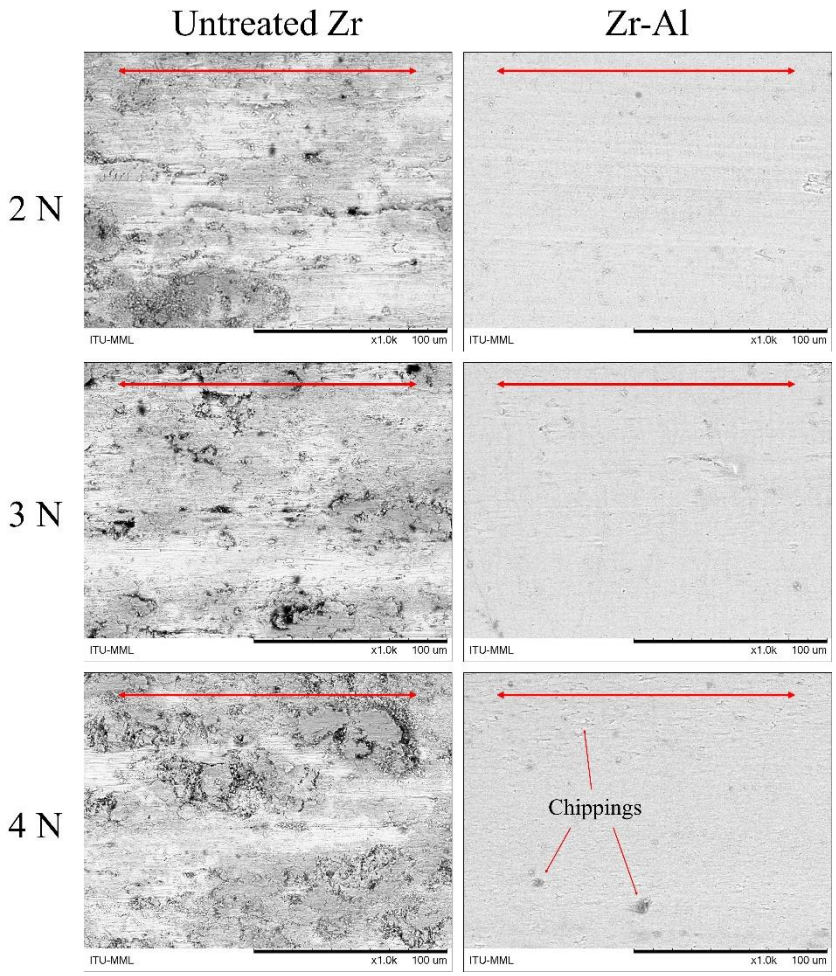

Figure 6. The wear track morphology of untreated Zr and Zr-Al samples under sliding 2, 3, and 4 N of loads.

The SEM micrographs of alumina counterface balls after testing for 2, 3, and 4 N of loads are given in Figure 7. It is evident that the balls slid against untreated Zr exhibited pronounced wear scars and material transfer. A dark metallic film was observed on the alumina ball when the test was applied under 4 N against untreated Zr samples, which indicated that detached metallic zirconium (and possibly its oxide) was deposited on the ball. During sliding, fragments of zirconium were pulled out of this transfer layer and adhered to the alumina surface. This not only removed material from the untreated Zr sample but also roughened the ball, which can contribute to third-body abrasion as the test progressed.

On the other hand, the alumina balls used against the surface of the Zr–Al sample were considerably cleaner. Even at 4 N, the ball showed only a mild circular wear track with faint discoloration and almost no visible metallic debris. There was little to no adhesive layer on the ball, which indicates that the hard intermetallic layer prevented significant material transfer. Any debris that formed was likely ejected from the contact or oxidized into fine particles that did not adhere to the surface. The smoother condition of the alumina counterface correlated with the more stable, lower friction behavior observed in the Zr-Al sample. The minimal material transfer caused by sliding occurred primarily between the alumina ball and the hard intermetallic layer, a combination that inherently yielded lower friction by limiting metallic adhesion. The findings of this study are similar to those of other hard coatings; for example, MAX-phase coatings on zirconium alloys result in cleaner counterfaces and less worn counterfaces, whereas uncoated alloys cause substantial material transfer and counterface wear [26]. A similar behavior was observed in another study [27], where extensive wear and a high wear rate (~6 mm^3/Nm) were recorded, with wear depths reaching 30 µm under all loads. Material transfer to the counterface and exposure of the Zr substrate highlighted the severe adhesive wear and inadequate surface integrity of the uncoated alloy.

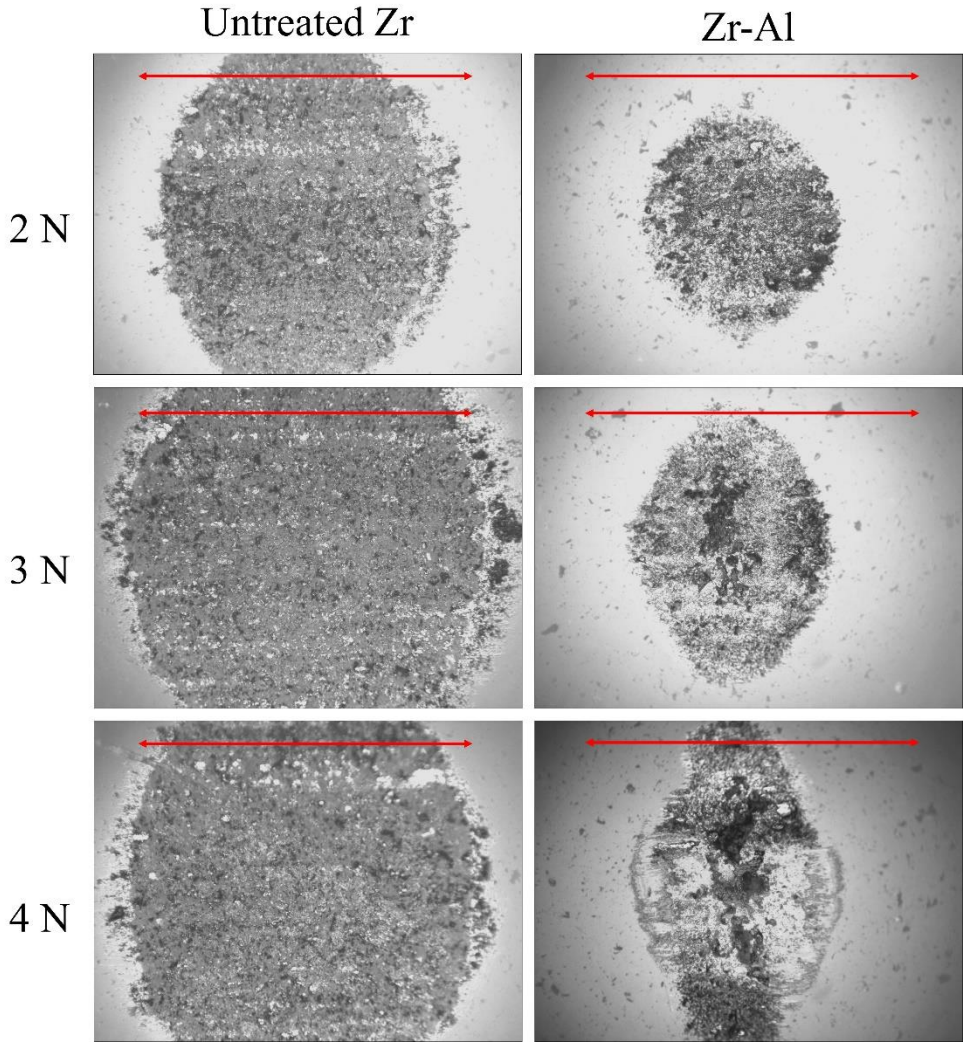

Figure 7. The counterface (alumina ball) morphology of untreated Zr and Zr-Al samples under sliding 2, 3, and 4 N of loads.

4. CONCLUSIONS

The present study demonstrates that pack aluminizing significantly improved the surface hardness and tribological performance of Zr 702 alloy. A continuous intermetallic layer (~40 µm thick) composed primarily of a Zr–Al compound (i.e. Al_3Zr) was formed on the surface. This intermetallic layer was dense, well-adhered, and significantly harder than the substrate, which effectively compensated for the relatively low hardness and

poor wear resistance of zirconium and its alloys. Accordingly, the aluminized Zr 702 exhibited enhanced wear resistance and reduced friction compared to the untreated Zr 702 sample. The key findings include:

- Pack aluminizing produced a uniform ~40 μm thick intermetallic layer that was continuous, adherent, and composed of Al_3Zr, as confirmed by XRD. This intermetallic layer was free of cracks, bonded well to the substrate and provided a hard surface.
- The aluminized surface reached a Vickers microhardness of 703.1 ± 76.7 HV0.025, nearly four times that of the untreated Zr sample (182.9 ± 20.7 HV0.025). Consequently, the Zr–Al sample displayed approximately 70% less wear volume under a 4 N load than the untreated Zr sample. Even under this highest load, the Zr-Al sample showed only a minimal, shallow wear track, whereas the untreated Zr sample suffered severe grooving and high material loss.
- The aluminized Zr–702 displayed a lower and more stable COF during sliding (steady-state COF ~0.35 vs ~0.6 for the untreated Zr at 4 N). A hard intermetallic layer on the surface prevented strong adhesion and material transfer to the alumina counterface, thereby reducing friction and virtually eliminating counterface damage. Accordingly, the dominant wear mechanism shifted from severe adhesive and abrasive wear in untreated Zr (with metallic transfer to the ball) to mild abrasive and oxidative wear in the Zr–Al sample.

In summary, this simple diffusion-based surface modification presents a promising approach to overcoming the wear limitations of zirconium and extending the service life of zirconium components in demanding tribological applications.

ACKNOWLEDGMENT

Dr. F. Muhaffel thanks Mr. E. Balci from Istanbul Technical University, Türkiye, for the technical assistance provided during the pack aluminizing of Zr 702 alloy. Dr. F. Muhaffel would also like to thank the support of the Turkish Academy of Sciences (TÜBA)—Outstanding Young Scientists Award (GEBİP).

REFERENCES

[1] R.B. Adamson, P. Rudling, Properties of zirconium alloys and their applications in light water reactors (LWRs), Woodhead Publishing Limited, 2013. https://doi.org/10.1533/9780857097453.2.151.

[2] J. Xu, H. Li, X. Zhao, J. Wu, B. Zhao, H. Zhao, J. Wu, Y. Zhang, C. Liu, Zirconium based neutron absorption material with outstanding corrosion resistance and mechanical properties, J. Nucl. Mater. 567 (2022) 153763. https://doi.org/10.1016/j.jnucmat.2022.153763.

[3] J. Jiang, C. Zhou, Y. Zhao, F. He, X. Wang, Journal of the Mechanical Behavior of Biomedical Materials Development and properties of dental Ti – Zr binary alloys, J. Mech. Behav. Biomed. Mater. 112 (2020) 104048. https://doi.org/10.1016/j.jmbbm.2020.104048.

[4] N.B. Bonnheim, D.W. Van Citters, M.D. Ries, L.A. Pruitt, Oxidized Zirconium Components Maintain a Smooth Articular Surface Except Following Hip Dislocation, J. Arthroplasty 36 (2021) 1437–1444. https://doi.org/10.1016/j.arth.2020.10.054.

[5] C. Hu, L. Chai, Z. Wang, T. Yang, Y. Tang, Z. Wang, W. Gong, K.L. Murty, Microstructure and wear resistance of zirconium manufactured by laser directed energy deposition, Int. J. Refract. Met. Hard Mater. 130 (2025) 107168. https://doi.org/10.1016/j.ijrmhm.2025.107168.

[6] X. Xiong, X. Li, J. Alexander, Z. Zhang, H. Dong, A Novel Catalytic Ceramic Conversion Treatment of Zr702 to Combat Wear, Materials (Basel). 16 (2023). https://doi.org/10.3390/ma16051763.

[7] S. Wang, Y. Zhang, H. Ming, J. Wang, J. Wang, E.H. Han, Impact of dissolved oxygen concentration on the coupling damage between fretting wear and corrosion on zirconium alloy cladding tube in high temperature pressurized water, Wear 572–573 (2025) 206058. https://doi.org/10.1016/j.wear.2025.206058.

[8] D. Zhu, X. Li, S. Chai, T.S. Chee, C. Kim, L. Li, D. Liu, Evaluation of wear, corrosion, and biocompatibility of a novel biomedical TiZr-based medium entropy alloy, J. Mech. Behav. Biomed. Mater. 165 (2025) 106951. https://doi.org/10.1016/j.jmbbm.2025.106951.

[9] N.C. Reger, V.K. Balla, M. Das, A.K. Bhargava, Wear and corrosion properties of in-situ grown zirconium nitride layers for implant applications, Surf. Coatings Technol. 334 (2018) 357–364. https://doi.org/10.1016/j.surfcoat.2017.11.064.

[10] V. Pawar, C. Weaver, S. Jani, Physical characterization of a new composition of oxidized zirconium-2.5 wt% niobium produced using a two step process for biomedical applications, Appl. Surf. Sci. 257 (2011) 6118–6124. https://doi.org/10.1016/j.apsusc.2011.02.014.

[11] R. V. Umretiya, B. Elward, D. Lee, M. Anderson, R.B. Rebak, J. V. Rojas, Mechanical and chemical properties of PVD and cold spray Cr-coatings on Zircaloy-4, J. Nucl. Mater. 541 (2020) 50–65. https://doi.org/10.1016/j.jnucmat.2020.152420.

[12] B. Maier, H. Yeom, G. Johnson, T. Dabney, J. Walters, J. Romero, H. Shah, P. Xu, K. Sridharan, Development of Cold Spray Coatings for Accident-Tolerant Fuel Cladding in Light Water Reactors, Jom 70 (2018) 198–202.

https://doi.org/10.1007/s11837-017-2643-9.
[13] H. Guan, L. Chai, X. Liu, Z. Li, G. Zhang, H. Wang, X. An, Microstructure, hardness and wear performance of quaternary CrNbTiZr refractory medium-entropy alloy coating fabricated on a commercial Zr alloy by pulsed laser cladding, J. Mater. Res. Technol. 24 (2023) 8877–8886. https://doi.org/10.1016/j.jmrt.2023.05.142.
[14] Y. Lu, Q. Shangguan, C. Huang, J. Pan, J. Zeng, A study on diffusion in hot-dip aluminizing, in: Adv. Mater. Res., 2010: pp. 1253–1256. https://doi.org/10.4028/www.scientific.net/AMR.97-101.1253.
[15] Y. Yürektürk, M. Baydoğan, Characterization of ferritic ductile iron subjected to successive aluminizing and austempering, Surf. Coatings Technol. 347 (2018) 142–149. https://doi.org/10.1016/j.surfcoat.2018.04.083.
[16] R. Sitek, Influence of the high-temperature aluminizing process on the microstructure and corrosion resistance of the IN 740H nickel superalloy, Vacuum 167 (2019) 554–563. https://doi.org/10.1016/j.vacuum.2018.08.047.
[17] S. Sheikh, L. Gan, X. Montero, H. Murakami, S. Guo, Forming protective alumina scale for ductile refractory high-entropy alloys via aluminizing, Intermetallics 123 (2020) 106838. https://doi.org/10.1016/j.intermet.2020.106838.
[18] R. Pretorius, T.K. Marais, C.C. Theron, Thin film compound phase formation sequence: An effective heat of formation model, Mater. Sci. Reports 10 (1993) 1–83. https://doi.org/10.1016/0920-2307(93)90003-W.
[19] A. Laik, K. Bhanumurthy, G.B. Kale, Intermetallics in the Zr-Al diffusion zone, Intermetallics 12 (2004) 69–74. https://doi.org/10.1016/j.intermet.2003.09.002.
[20] A. Priyadarshi, T. Subroto, J. Nohava, S. Pavel, M. Conte, K. Pericleous, D. Eskin, I. Tzanakis, Investigation of mechanical properties of Al3Zr intermetallics at room and elevated temperatures using nanoindentation, Intermetallics 154 (2023) 107825. https://doi.org/10.1016/j.intermet.2023.107825.
[21] R. Priya, C. Mallika, U.K. Mudali, Wear and tribocorrosion behaviour of 304L SS, Zr-702, Zircaloy-4 and Ti-grade2, Wear 310 (2014) 90–100. https://doi.org/10.1016/j.wear.2013.11.051.
[22] K.M. Doleker, T. Yener, A. Erdogan, F. Yılmaz, G.C. Efe, Effect of Si and Cr on formation of aluminide coatings on Ti6Al4V alloy by low temperature aluminizing: Wear and oxidation behavior, Surf. Coatings Technol. 509 (2025). https://doi.org/10.1016/j.surfcoat.2025.132207.
[23] X. Wang, D. Qu, Y. Duan, M. Peng, Wear and corrosion properties of a B–Al composite layer on pure titanium, Ceram. Int. 48 (2022) 12038–12047. https://doi.org/10.1016/j.ceramint.2022.01.061.
[24] Y. Guo, Z. Wang, N. Li, S. Yang, Y. Wu, Y. Duan, A. Yang, L. Ma, S. Zheng, Y. Li, Microstructure , wear and corrosion behaviors of TC21 titanium alloy by solid powder-packing boriding and aluminizing, 36 (2025) 6387–6399. https://doi.org/10.1016/j.jmrt.2025.04.280.
[25] U. Gürol, Y. Altınay, A. Günen, Ö.S. Bölükbaşı, M. Koçak, G. Çam, Effect of powder-pack aluminizing on microstructure and oxidation resistance of wire arc additively manufactured stainless steels, Surf. Coatings Technol. 468 (2023). https://doi.org/10.1016/j.surfcoat.2023.129742.
[26] C. Tang, M. Stueber, H.J. Seifert, M. Steinbrueck, Protective coatings on zirconium-based alloys as accident-Tolerant fuel (ATF) claddings, Corros. Rev. 35 (2017) 141–165. https://doi.org/10.1515/corrrev-2017-0010.
[27] T.R. Netto, A. K. Evans, D. T. Goddard, J. L. Cooper, P. Kelly, Effects of sample bias on wear resistance of magnetron sputtered chromium coated zirconium alloy, Surf. Coatings Technol. 498 (2025) 131847. https://doi.org/10.1016/j.surfcoat.2025.131847.